



## RESEARCH ARTICLE

# Feature enhancement framework for brain tumor segmentation and classification

Bilal Tahir<sup>1</sup> | Sajid Iqbal<sup>1,2</sup>  | M. Usman Ghani Khan<sup>1</sup> | Tanzila Saba<sup>3</sup>  |  
Zahid Mehmood<sup>4</sup> | Adeel Anjum<sup>5</sup> | Toqeer Mahmood<sup>6</sup>

<sup>1</sup>Department of Computer Science and Engineering, University of Engineering and Technology, Lahore, Pakistan

<sup>2</sup>Department of Computer Science, Bahauddin Zakariya University, Multan, Pakistan

<sup>3</sup>Department of Information Systems, College of Computer and Information Sciences, Prince Sultan University Riyadh, Saudi Arabia

<sup>4</sup>Department of Software Engineering, University of Engineering and Technology, Taxila, Pakistan

<sup>5</sup>Department of Computer Science, COMSATS University, Islamabad, Pakistan

<sup>6</sup>Department of Computer Science, University of Engineering and Technology, Taxila, Pakistan

## Correspondence

Sajid Iqbal,  
Department of Computer Science, Bahauddin Zakariya University, Multan, Pakistan.  
Email: sajid.iqbal@bzu.edu.pk

Review Editor: Paolo Bianchini

## Funding information

Prince Sultan University Riyadh Saudi Arabia,  
Grant/Award Number: RG-CCIS-2017-06-02

## Abstract

Automatic medical image analysis is one of the key tasks being used by the medical community for disease diagnosis and treatment planning. Statistical methods are the major algorithms used and consist of few steps including preprocessing, feature extraction, segmentation, and classification. Performance of such statistical methods is an important factor for their successful adaptation. The results of these algorithms depend on the quality of images fed to the processing pipeline: better the images, higher the results. Preprocessing is the pipeline phase that attempts to improve the quality of images before applying the chosen statistical method. In this work, popular preprocessing techniques are investigated from different perspectives where these preprocessing techniques are grouped into three main categories: noise removal, contrast enhancement, and edge detection. All possible combinations of these techniques are formed and applied on different image sets which are then passed to a predefined pipeline of feature extraction, segmentation, and classification. Classification results are calculated using three different measures: accuracy, sensitivity, and specificity while segmentation results are calculated using dice similarity score. Statistics of five high scoring combinations are reported for each data set. Experimental results show that application of proper preprocessing techniques could improve the classification and segmentation results to a greater extent. However, the combinations of these techniques depend on the characteristics and type of data set used.

## KEYWORDS

BRATS data set, dice coefficient, image preprocessing, tumor classification, tumor segmentation

## 1 | INTRODUCTION

Tumor is unusual growth of body cells which are divided mainly into benign (noncancerous) and malignant (cancerous) types. Different types of tumors are classified into different categories by researchers (Rehman, Abbas, Saba, Mahmood, & Kolivand, 2018; Rehman et al., 2018; Saba, Rehman, Mehmood, Kolivand, & Sharif, 2018). Various researchers have used different characteristics of tumors to classify them (Fahad, Ghani Khan, Saba, Rehman, & Iqbal, 2018; Iqbal, Ghani, Saba, & Rehman, 2018; Iqbal, Khan, Saba, & Rehman, 2017; Mughal, Muhammad, Sharif, Rehman, & Saba, 2018; Mughal, Sharif, Muhammad, & Saba, 2017; Rehman, Abbas, Saba, Mahmood, & Kolivand, 2018; Rehman, Abbas, Saba, Mehmood, et al., 2018; Rehman et al., 2018; Sadad, Munir,

Saba, & Hussain, 2018). WHO categorization is considered to be the standard in the world. WHO categorizes the brain tumor into 120+ categories with 20 main categories and subcategories. Each tumor is graded among four types depending upon its level of severity (Louis et al., 2014). WHO classifies lung cancer into two main classes, small lung cancer and nonsmall lung cancer, with four stages of each type (Travis, 2015). Medical treatment of these tumors requires a proper diagnosis of tumor type and its grade (Mughal et al., 2017).

Medical imaging is the process of creating a visualization of the interior of human body parts for diagnosis at earlier stages and acquired images may be used in treatment at later stages and even after treatment for post-treatment results verification (Abbas et al., 2016; Abbas et al., 2018; Saba, Bokhari, Sharif, Yasmin, & Raza, 2018).

Many different techniques for medical imaging like CAT, X-ray, PET, and MRI, and so forth, are used by medical practitioners which are divided into two main categories: invasive and noninvasive (Aribandi, McCoy, & Bazan, 2007). Invasive imaging techniques are those which can damage human body parts whereas noninvasive techniques are considered safe. Although noninvasive techniques are safer, however, the role of invasive and noninvasive techniques is still debatable (Dolic et al., 2013). Therefore, we considered noninvasive techniques only in this study.

MRI has evolved as a popular noninvasive technique for brain imaging because it provides high-resolution spatial images and gives high contrast values for soft tissues (Iqbal et al., 2017; Iqbal et al., 2018) while CT scan is the more preferred approach for lung cancer diagnosis (Wever, Coolen, & Verschakelen, 2011). Current research shows the importance of medical images in diagnosis, treatment, and monitoring of treatment results (Houshmand, Werner, & Alavi, 2016; Yang et al., 2016; Mughal et al., 2018).

Medical image-based diagnosis of tumor is mainly performed using computational techniques known as a classification that sorts images into benign and malignant categories. Researchers are also using image classification tasks to grade tumor in medical images (Louis et al., 2014). Tumor classification is still a challenging problem for image processing researchers because many tumor cells feature like area, contrast, and structure around the tumor cell show similar patterns (Justin et al., 2017). The classification process consists of preprocessing, segmentation, feature extraction, feature reduction, and classification.

Preprocessing is an optional phase used to improve the quality of available images before feeding them to the classification/segmentation pipeline. These preprocessed images can boost the results of classification/segmentation algorithms by helping in the extraction of high-value features and filter out low-value features (Kumar & Karnan, 2014). This phase may consist of skull striping (Bandhyopadhyay, 2012), noise removal (Jamal, Hazim Alkawaz, Rehman, & Saba, 2017), eddy current effect removal (Simonetti et al., 2003), band reduction limit (Vidyarthi, Agarwal, & Mittal, 2014), image restoration and image standardization (Chaddad, 2015).

It is known that segmentation, feature extraction, feature selection, and classification algorithms have a substantial impact on medical image-based diagnosis process. However, preprocessing steps may also improve the performance if applied suitably. In this article, impact different preprocessing techniques on tumor classification and segmentation is studied. A framework of preprocessing techniques is developed and applied to different data sets. Popular preprocessing techniques like noise removal, edge enhancement, and histogram enhancement are applied on data sets one by one before segmentation and classification. The final results of experiments are evaluated to find out optimality of various preprocessing techniques.

Rest of the article is organized as follow: Section 2 explores related state of the art. Proposed preprocessing techniques used in the experiments are presented in Section 3. Section 4 describes the materials and methods. In Section 5, experimental results are exhibited. Finally discussion and conclusion is presented in Section 6.

## 2 | STATE OF THE ART

Medical imaging research community has been using preprocessing techniques at large to increase the performance and confidence score of their designed methods. Different researchers have experimented different preprocessing techniques for segmentation and classification of medical images. Hussein et al. (2009) deployed median filter followed by morphological operations followed by Contrast enhancement to see the effect of preprocessing on contour detection from echocardiograph images. They showed that preprocessing can significantly improve the contour detection. Median filter with large window size has more effective results as it provides more noise reduction and less blurring effect (Perona & Malik 1990). Denoising techniques of the Gaussian filter, anisotropic diffusion, nonlocal means (NLM), denoising, and wavelet techniques are deployed by Diaz et al. (2011) before segmentation. The results showed the best performance of nonlocal means denoising algorithm followed by wavelet and anisotropic diffusion with good results. The impact of wavelet denoising algorithm is observed by Li, Li, Zhu, and Kambhamettu (2002). Their experiment has two parts, first part used to observe the impact of wavelet denoising on different classifiers and second part observed the effect of wavelet denoising on different data sets. The results showed significant improvement in classification where temporal or spatial localities exist. Wavelet coefficients cannot characterize the noise where localities are weak or did not exist.

Patil and Udupi (2012) investigated the impact of preprocessing on MRI and CT scans of thorax, abdomen and brain with tumor. Median filter followed by skull/ribcage removal and morphological operations were applied to images. The final results were observed visually showing the acceptable results on brain MR images as artifacts and unwanted areas were removed successfully. In case of CT scan of thorax, abdomen and brain artifacts were removed successfully but brain skull was not completely removed however thinned and ribcage effect in thorax and abdomen scans was minimized significantly. Mittal and Anand (2013) used different morphological filters, that is, Sobel, Gaussian, Prewitt, LoG, Gaussian, disk, average, and Laplacian filters on images before watershed-based segmentation. Results for denoising, using peak-signal to noise ratio (PSNR), mean square error (MSE) showed that motion, disk, and Gaussian filters had best whereas Sobel and Prewitt's filters produced poor results. However, in case of segmentation, Sobel and Prewitt produced best results. Authors showed that Sobel and Prewitt had good results when segmentation and denoising were considered overall. The final results of each filter depend on image quality to be segmented and denoised. Median, adaptive median, mean, and Weiner filters are applied to remove noise from mammography images by Ramani, Vanitha, and Valarmathy (2013). The comparison of filter results was done using parameters of PSNR, MSE, structural (SC), and normalized absolute error (NAE). The values of parameters show the overall best performance of median filter. Gaussian, mean, bilateral filter, Gabor filter, Laplacian, and high-pass filters are applied by Vijaya & Suhasini (2014) applied on CT scan lung images to observe effect of filters on images. Final results were shown in values of PSNR and NAE values. The tabular values of results show the best result of bilateral filter

**TABLE 1** Preprocessing techniques used in reviewed work and proposed method

Work	Noise removal					Histogram equalization					Edge enhancement					
	GF	ANS	WD	BF	GBF	MF	WF	MDF	HE	MHE	LP	USM	SEG	MSS	MDS	CLF
Li et al., 2002			X												X	X
Hussein et al., 2009								X		X						
Diaz et al., 2011	X	X	X													
Patil et al. 2012					X	X	X	X						X	X	
Ramani et al., 2013						X		X					X			
Vijaya et al. 2014	X				X	X	X									
Lone et al. 2015			X			X	X	X								
Proposed work	X	X	X	X	X	X	X	X	X	X	X	X	X	X	X	X

**GF** = Gaussian filter[29]; **ANS** = Anisotropic diffusion[41]; **WD** = Wavelet denoising[45]; **BF** = Bilateral filter denoising[49]; **GBF** = Gabor filter[34]; **MF** = Mean filter[22]; **WF** = Wiener filter[6]; **MDF** = Median filter[20]; **HE** = Histogram equalization[54]; **MHE** = Multihistogram equalization[54]; **LP** = Laplacian edge enhancement[42]; **USM** = Un-sharp Masking[42]; **MSS** = Multiscan schemes; **MDS** = Multidata sets; **CLF** = Classification.

whereas high pass, Laplacian and Gabor filters have worst results. The alpha-trimmed mean filter performs well after bilateral filter. Lone and Malik (2015) deployed median, mean, Wiener filter, and wavelet denoising to medical images. Gaussian noise, salt and pepper noise, and speckle noise are added into image and then filters are applied. PSNR and MSE values are used to compare the results. Results show the outperformance of wavelet to spatial filters as spatial filters have constraints of degrading, deblurring, and edge destruction. Among spatial filters values show the best performance of Wiener filter.

Preprocessing techniques are mainly divided among three groups: noise removal, histogram equalization, and edge enhancement. Table 1 lists the comparative view of reviewed work. Last four columns show the optional steps performed in reviewed work. In last row, we present our own scheme to analyze the effect of preprocessing techniques.

### 3 | PREPROCESSING METHODS

Preprocessing methods for denoising, edge enhancement, and histogram enhancements are applied before processing medical images for diagnosis purpose. Wavelet denoising is used to remove the noise from image while preserving its characteristics regardless of frequency component (Husham, Alkawaz, Saba, Rehman, & Alghamdi, 2016). It consists of three steps of wavelet transform, thresholding, and finally inverse wavelet transform.

Wavelet and inverse wavelet transforms are linear but thresholding is nonlinear process. Entire denoising process is heavily dependent on thresholding parameters and values (Jansen, 2012). Bilateral Filter is nonlinear filter which preserves edges while smoothing the image (Manduchi, 1998). It combines pixel values based on their geometric

distance and photometric values preferring near values than distant values. Bilateral filter operates on all bands at once resulting in no phantom effect on edges. Gabor based denoising include the process of transforming the image into Gabor domain, thresholding the Gabor coefficients and finally taking inverse transform of coefficients to obtain denoised image. The quality of denoising depends on thresholding technique used to find threshold values (Nezamoddini-Kachouie & Fieguth, 2005). Low threshold value did not remove noise and high threshold value blurs the image. Gaussian filter removes noise by smoothing the image. The main feature of Gaussian filter is to follow curve and level of smoothness depend on variance of Gaussian filter.

Mean filter defines a window of fixed size and then calculates the value of central point as the mean of all neighboring pixels. Final results depend on size of the filter but as size of filter increases, image sharpness and high-frequency component details are lost. Median filter simply replaces the target pixel value with the median of neighboring pixels. It is more effective than mean filter in salt and pepper noise because it does not blur edges. Sharp details are preserved during filtering as filter is independent of value of neighborhood pixels (Jain & Schunck, 1995). Wiener filter reduces the noise by estimating the power spectrum of image and noise. Mean and variance of each pixel is calculated using neighbor pixels to create a pixel-wise wiener filter. Wiener filter performance is dependent on calculation of spectrum of noise and image. Noise and image power calculation is difficult task due to same power spectrum of different images (Chen et al., 2006).

Histogram equalization enhances brightness of image by normalizing the image intensity distribution by cumulative distribution function. In some cases histogram equalization create wash-out effect by average of intensities to the middle (Zuiderveld, 1994). Multihistogram

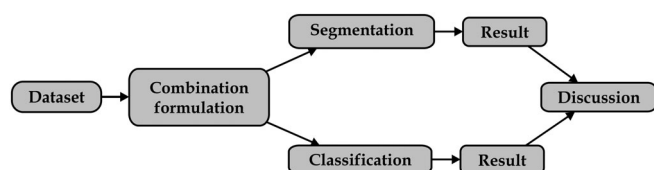
**FIGURE 1** Proposed research framework**TABLE 2** Data sets and their properties for binary classification

Image set	Imaging modality	Total images	Number of patients	Number of studies
IS-1 lung cancer	CT	22,489	70	70
IS-2 brain cancer	MRI	81,325	49	52
IS-3 BRATS images	MRI	469	300	

**TABLE 3** Example combinations of preprocessing techniques

S#	Noise removal	Contrast enhancement	Edge enhancement
1	GF	HE	LP
2	ANS	HE	UNM
3	WF	MHE	LP

**TABLE 4** Data sets division between training and test sets for classification

Image set	Image set division	
	Training set size	Test set size
IS-1	20,241	2,248
IS-2	1920	214
IS-3	422	47

equalization (MHE) is process of dividing image into subimages and equalize the histogram of each sub image and merge them to get final equalized image. The MHE prevents the procedure of over equalization (Yoon, Han, & Hahn, 2009).

Laplacian edge enhancement or unsharp masking are techniques in which filtered image, a scaled version of original image is added into original image to enhance the high-frequency components. Techniques perform well in many applications but the tradeoff between noise enhancement and edge enhancement during process needs to be considered (Polesel, Ramponi, & Mathews, 2000).

## 4 | MATERIALS AND METHODS

The proposed study consists of the following main components: data set selection, combination formulation, application of preprocessing techniques, and segmentation/classification. The flow chart of the study is exhibited in Figure 1.

### 4.1 | Benchmark data set

To evaluate the impact of preprocessing techniques on medical images classification, three different data sets obtained through non-invasive modalities that is, MRI and CT are used. These image-sets include Lung CT scans (Armato et al., 2015), Brain MRI (Cheng et al., 2015), and BRATS images (Menze et al., 2015). The description of these data sets is given in Table 2.

Selected preprocessing techniques are divided among three groups: noise removal, edge enhancement, and contrast enhancement. The implementation process work in two phases: combination formulation and their application on selected data sets. Thirty-three unique combinations are formed in the first phase. Each combination is formed by taking one technique from each group that is, the first combination is (GF, HE, LP). In the second phase, they are applied in order on each data set. For example, in combination (GH, HE, LP), GH is

**TABLE 6** IS-1 results for classification

Combination	Acc	Spec	Sens
GF + HE + UNM	0.83	0.90	0.72
MF + MHE + UNM	0.83	0.89	0.73
MDF + HE + UNM	0.82	0.89	0.71
BIF + MHE + LP	0.81	0.88	0.71
ANS + HE + UNM	0.80	0.86	0.73
NO preprocessing	0.72	0.76	0.67

**TABLE 7** IS-2 results for classification

Combination	Acc	Spec	Sens
MF + HE + UNM	0.86	0.91	0.79
GF + HE + UNM	0.85	0.91	0.79
MDF + MHE + LP	0.85	0.90	0.79
ANS + MHE + LAP	0.84	0.90	0.77
GF + MHE + UNM	0.84	0.90	0.77
NO preprocessing	0.72	0.80	0.60

**TABLE 8** IS-3 results for classification

Combination	Acc	Spec	Sens
MF + HE + LP	0.82	0.89	0.73
MDF + MHE + UNM	0.80	0.87	0.71
MDF + MHE + LP	0.80	0.87	0.71
GBF + HE + LP	0.79	0.85	0.71
ANS + HE + UNM	0.77	0.84	0.71
NO preprocessing	0.62	0.74	0.50

applied first followed by HE and finally LP. Table 3 lists a few of these combinations.

### 4.2 | Classification

Classification is the task of labeling the images according to a class of tumor. Classification task consists of preprocessing, segmentation, feature extraction, and classification. Preprocessing techniques are applied as described in Section 4.2.

To find the unbiased results, for the first task, we have used a simple image segmentation method known as Otsu method based on thresholding of pixels (Otsu, 1975). Otsu thresholding works considering that image to be thresholded consists of two groups of pixels and evaluate the optimal threshold point so that the intraclass variance of two groups is negligible.

In next phase, segmented images are used to calculate the 2D discrete wavelet transform using Daubechies wavelets base and produced features are reduced using principal component analysis (PCA)

**TABLE 5** Data sets' statics for binary segmentation

Image set	Data set size	T1 samples	T1c samples	T2 samples	Flair sample
BRATS-2015	72,208	18,072	18,052	18,050	18,034
BRATS-2016	72,202	18,070	18,049	18,052	18,031

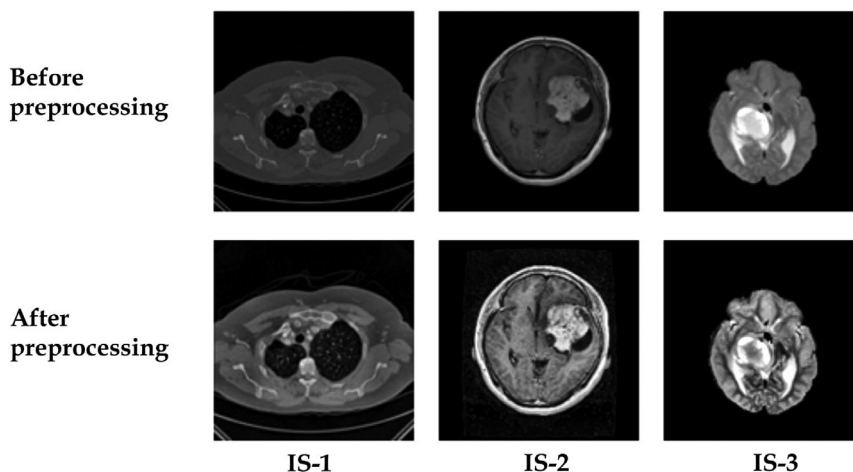


**FIGURE 2** Sample images used for classification. Before preprocessing (top row) vs after preprocessing (bottom row)

technique (Fodor, 2002). It has been observed by researchers that application of PCA reduces results accuracy in classification phase, however, this technique is applied to all image sets so there is the equal impact of the application of PCA. Values calculated through DWT are used to form grey level co-occurrence matrix (Haralick, Shanmugam, & Dinstein, 1973) and finally different spatial properties of images are derived. The derived features include energy, contrast, correlation, homogeneity, inverse difference matrix, and entropy.

For the second task, image classification, linear binary classifier support vector machine (SVM) (Cortes & Vapnik, 1995) is used. SVM has been intensively studied and benchmarked against a variety of techniques and is one of the best classification techniques that have computational advantages over other techniques (Cristianini & Shawe-Taylor, 2000). We have applied supervised learning method in which SVM works in two phases. In first phase, the model is trained against the labeled features provided and in second phase, test image set is used to find out trained model predictions. Breakup of data sets for training and test is given in Table 4.

**TABLE 9** T1 modality results for segmentation of BRATS 15

	DSC	r
GF + HE + UNM	0.78	0.72
MF + HE + LAP	0.78	0.71
GF + HE + UNM	0.77	0.72
GF + MHE + LAP	0.77	0.72
WF + HE + UNM	0.76	0.70
No preprocessing	0.63	0.51

**TABLE 10** T1c modality results for segmentation of BRATS 15

	DSC	r
GF + MHE + UNM	0.80	0.74
GF + HE + UNM	0.79	0.73
MF + MHE + LP	0.77	0.71
GBF + MHE + UNM	0.76	0.72
WF + HE + LP	0.76	0.71
No preprocessing	0.65	0.53

Usually training error reduces with increase in training, however, test error shows different pattern. It reduces to some extent of test set and then starts increasing again (Kearns, 1997). The data distribution in test set is unpredictable to a certain degree. To measure the system performance in better way, cross-validation is used. We also use 10-fold cross-validation. The results than obtained are averaged.

$$\epsilon_{\text{test}} = \left( \frac{1}{m} \right) \left( \frac{1}{n} \right) \sum_i^m \sum_j^n (y_{ij} = y'_{ij}) \quad (= 1 \forall y \neq y') \text{ and } (= 0 \forall y = y')$$

where

$y$  = actual class of image,  $y'$  = predicted class of image.

$i$  = index of image in particular cross validation  $j$  = index of cross validation set

### 4.3 | Segmentation

To evaluate the segmentation performance in supervised learning, ground truth (segmented) image are required (Jamal et al., 2017). The BRATS is only data sets in our study which has well-defined ground

**TABLE 11** T2 modality results for segmentation of BRATS 15

	DSC	r
GF + HE + UNM	0.81	0.74
MDF + HE + UNM	0.80	0.75
MF + MHE + UNM	0.80	0.73
ANS + MHE + LP	0.78	0.71
WF + HE + LP	0.77	0.69
No preprocessing	0.69	0.58

**TABLE 12** Flair modality results for segmentation of BRATS 15

	DSC	r
MF + HE + LP	0.84	0.77
GF + HE + UNM	0.84	0.72
GBF + HE + UNM	0.83	0.70
MDF + HE + LP	0.80	0.73
GF + MHE + UNM	0.80	0.69
No preprocessing	0.70	0.58

**TABLE 13** T1 modality results for segmentation of BRATS 16

	DSC	r
MF + HE + UNM	0.80	0.72
GF + HE + UNM	0.78	0.71
GF + MHE + LP	0.78	0.69
MDF + MHE + LAP	0.76	0.68
WF + HE + UNM	0.75	0.70
No preprocessing	0.64	0.53

**TABLE 14** T1c modality results for segmentation of BRATS 16

	DSC	r
GF + MHE + UNM	0.81	0.70
GF + HE + LP	0.80	0.70
MDF + MHE + UNM	0.80	0.69
GBF + MHE + UNM	0.77	0.70
WF + HE + LP	0.76	0.72
No preprocessing	0.64	0.54

truth images for segmentation. So, we only consider BRATS as a data set in segmentation phase. Three dimensional images are converted into slices of 2D images and to remove the redundant information only those slices are considered which have more than 100 non-zero pixels. The statistics of the data set can be viewed in the Table 5 The combination of preprocessing is deployed in same manners as it is done in image classification phase. There is a large number of segmentation

techniques (Paulinas & Ušinskas, 2015; Zhang, 1996) formulated by researchers. We have used a simple image segmentation method known as Otsu method based on thresholding of pixels (Otsu, 1975). Image segmentation was done using a static method so it does not require any training of machine learning algorithm. The data set statistics can be viewed in the Table 5.

## 5 | EXPERIMENTAL RESULTS

### 5.1 | Classification results

To analyze the classification efficiency, we use three different measures which are used widely. Accuracy, sensitivity, and specificity below listed formulas are used to calculate accuracy (acc), sensitivity (sens), and specificity (spec).

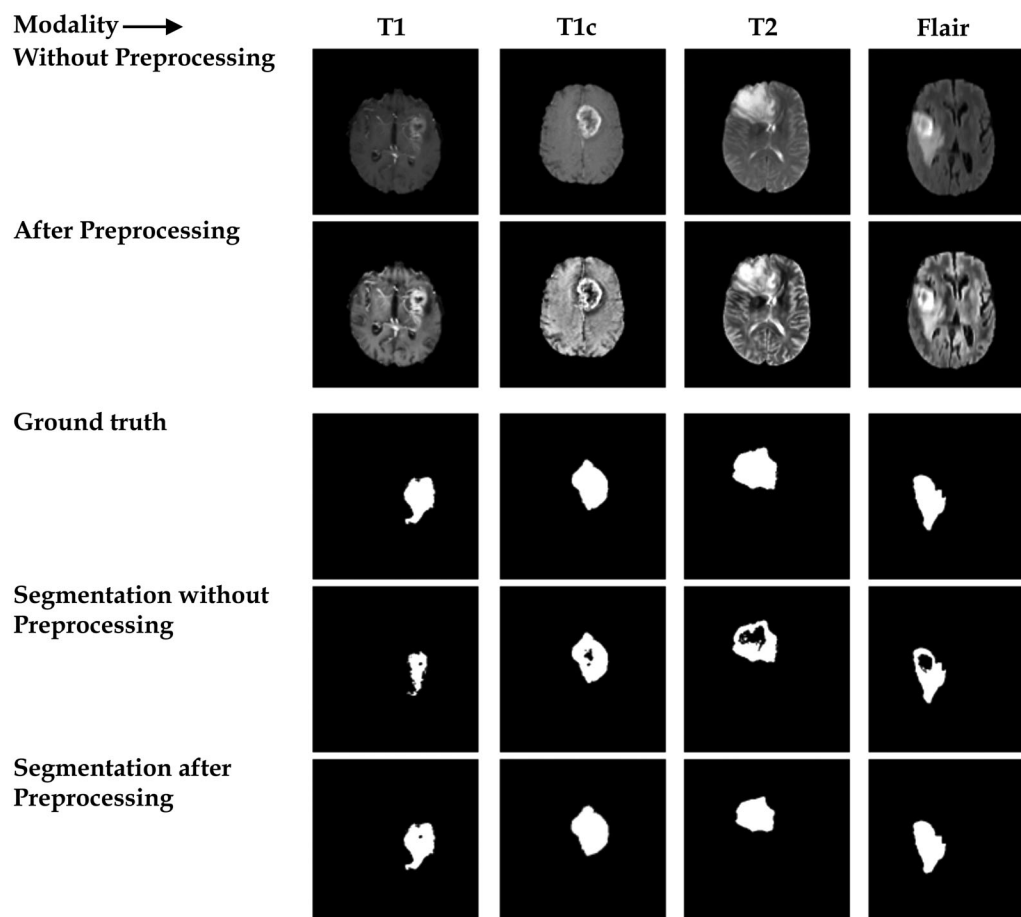
$$\text{Accuracy} = (TP + TN)/(P + N)$$

$$\text{Sensitivity} = (TP)/(TP + FN)$$

$$\text{Specificity} = (TN)/(FP + TN)$$

The results produced during experiments for each image set with five top scoring preprocessing combinations are shown in Tables 6–8.

Values of accuracy, specificity, and sensitivity of best five combinations of preprocessing techniques are reported. It can clearly be noticed from results that accuracy and specificity increase due to

**FIGURE 3** Segmentation results on BRATS 2015 data set before and after preprocessing



**TABLE 15** T2 modality results for segmentation of BRATS 16

	DSC	r
MDF + HE + UNM	0.79	0.68
GF + HE + LP	0.77	0.70
GF + MHE + UNM	0.77	0.69
MD + HE + LP	0.76	0.66
ANS + HE + LP	0.76	0.67
No preprocessing	0.69	0.60

preprocessing of data. Figure 2 shows the images before and after applying preprocessing combinations of data sets under study.

## 5.2 | Segmentation results

Evaluation of segmentation result is done using dice similarity coefficient(DSC) and recall(r). Dice similarity measures the overlap area of two images using following equation.

$$DSC(im1, im2) = \frac{2(im1 \cap im2)}{im1 \cup im2}$$

Where im1 and im2 are two images to be compared.  $\cap$  and  $\cup$  can be operated as "logical and" and "logical or" operations, respectively. The results of the top five best performing techniques on each modality can be viewed in the Tables 9–12 (for BRATS 2015) and 13, 14,

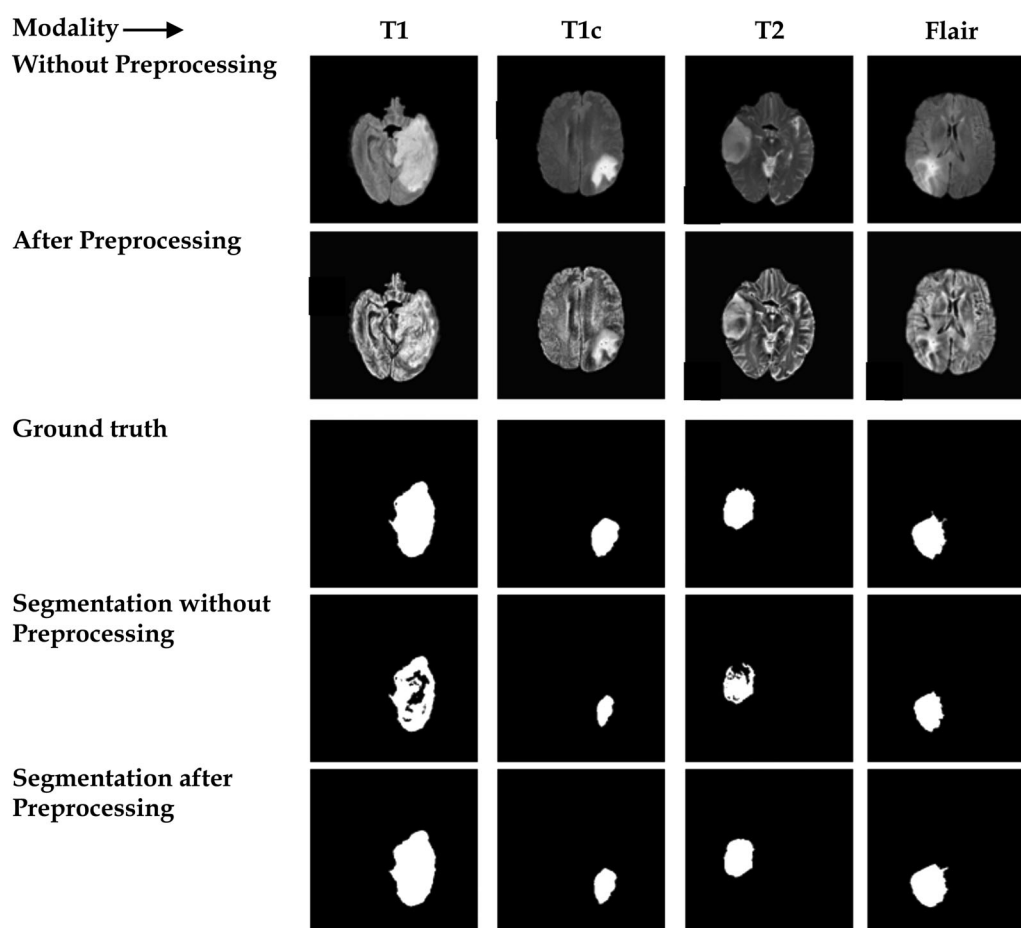
**TABLE 16** Flair modality results for segmentation of BRATS 16

	DSC	r
MF + HE + LP	0.83	0.74
GF + HE + LP	0.81	0.70
GF + MHE + UNM	0.81	0.69
WF + HE + LP	0.76	0.70
GBF + HE + UNM	0.77	0.71
No preprocessing	0.61	0.50

15, and 16 (for BRATS 2016). Improvement in segmentation results is shown in Figure 3 for BRATS 2015 and in Figure 4 for BRATS 2016.

## 6 | DISCUSSION AND CONCLUSION

In this work, the impact of popular preprocessing techniques has been examined using different data sets of medical images produced through noninvasive imaging modalities. Preprocessing techniques are divided into three main categories: noise removal, contrast enhancement, and edge detection. Use of a combination of different preprocessing techniques is more beneficial than applying the single preprocessing technique. The analysis is done by forming all possible combinations of preprocessing techniques categorizing them among three categories using three different image sets.

**FIGURE 4** Segmentation results on BRATS 2016 data set before and after preprocessing

**TABLE 17** Top performer preprocessing techniques for all data sets for classification

Category	Technique
Noise removal	MF, GF
Contrast enhancement	HE
Edge enhancement	UNM

**TABLE 18** Top performer preprocessing techniques for all data sets for segmentation

Category	Technique
Noise removal	GF, MF
Contrast enhancement	HE
Edge enhancement	UNM

The extensive experimental analysis shows that application of preprocessing techniques is an important step and can improve results to a considerable extent in medical image analysis tasks including classification and segmentation as shown in resulting Tables 9–16.

We found that appropriate combination of preprocessing techniques depends upon the data set and imaging modality. There is no unique combination of such preprocessing techniques that can perform better for all image sets. A combination of GF, HE, and UNM outperform for IS-1 and IS-2 but for IS-3 these combination results are poor. Combination of GBF, MHE, and UNM has a good result for IS-1 and IS-3 but for IS-2 combination results are not considerable.

However, the role of individual preprocessing techniques can suggest the choice of a particular preprocessing combination. For IS-1, in noise removal, GF, for contrast enhancement, HE and for edge enhancement, UNM have outperformed. For IS-2, results show that among winners are MF, HE, and UNM and finally for IS-3, results obtained show that MF, HE, and LP are in leading preprocessing techniques.

For segmentation results, GBF and GF with a combination of HE and UNM outperformed the other techniques as these are present in top results of all four types of modalities. WF also improves the similarity score by making a different combination with histogram equalization and edge enhancement technique. HE and UNM provide more promising results than other enhancement techniques. Considering the results of applications of different combinations of preprocessing techniques for medical image segmentation, techniques producing better results are given in Table 18.

To measure the performance of classification algorithm, three widely used metrics are calculated: accuracy, sensitivity, and specificity. The sensitivity of results for each image set is found almost similar for different combinations of preprocessing techniques, however, there is observable variation in accuracy and specificity. Hence, these two measures are distinguishing metrics of more useful combinations of preprocessing techniques.

The measurement of segmentation results is done by finding the dice similarity score of segmented and ground truth images. The segmentation results in all modalities remain consistent and few combinations of preprocessing techniques outperformed the others.

As a variety of image sets are used in this study, the results obtained could be generalized for other image sets of noninvasive imaging modalities. Researchers can explore the applications of these techniques using different permutations with more data sets. As a future work, we intend to explore the impact of preprocessing for multiclass classification and segmentation.

## ACKNOWLEDGMENT

This work is supported by the Machine Learning Research Group; Prince Sultan University Riyadh; Saudi Arabia [RG-CCIS-2017-06-02]. The authors are grateful for this support.

## ORCID

Sajid Iqbal  <https://orcid.org/0000-0003-1760-7653>

Tanzila Saba  <https://orcid.org/0000-0003-3138-3801>

## REFERENCES

- Abbas, N., Saba, T., Rehman, A., Mehmood, Z., Kolivand, H., Uddin, M., & Anjum, A. (2018). Plasmodium life cycle stage classification based quantification of malaria parasitaemia in thin blood smears. *Microscopy Research and Technique*. <https://doi.org/10.1002/jemt.23170>
- Abbas, N., Saba, T., Mohamad, D., Rehman, A., Almazayad, A. S., & Al-Ghamdi, J. S. (2016). Machine aided malaria parasitemia detection in Giemsa-stained thin blood smears. *Neural Computing and Applications*, 29(3), 803–818. <https://doi.org/10.1007/s00521-016-2474-6>
- Aribandi, M., McCoy, V. A., & Bazan, C. (2007). Imaging features of invasive and noninvasive fungal sinusitis: A review 1. *Radiographics*, 27(5), 1283–1296.
- Armato, S. G., III, et al. (2015). *SPIE-AAPM-NCI lung nodule classification challenge dataset*. CA, US: Cancer Imaging Arch.
- Chaddad, A. (2015). Automated feature extraction in brain tumor by magnetic resonance imaging using gaussian mixture models. *Journal of Biomedical Imaging*, 2015, 8.
- Chen, J., Benesty, J., Huang, Y., & Doclo, S. (2006). New insights into the noise reduction Wiener filter. *IEEE Transactions on Audio, Speech, and Language Processing*, 14(4), 1218–1234.
- Cheng, J., Huang, W., Cao, S., Yang, R., Yang, W., Yun, Z., ... Feng, Q. (2015). Enhanced performance of brain tumor classification via tumor region augmentation and partition. *PloS One*, 10(10), e0140381.
- Cortes, C., & Vapnik, V. (1995). Support-vector networks. *Machine Learning*, 20(3), 273–297.
- Cristianini, R. N., & Shawe-Taylor, J. *An introduction to support vector machines and other kernel-based learning methods*. Cambridge University Press, 2000.
- Diaz, I., Boulanger, P., Greiner, R., & Murtha, A. (2011). A critical review of the effects of de-noising algorithms on MRI brain tumor segmentation. Paper presented at the IEEE Annual International Conference of the Engineering in Medicine and Biology Society, pp. 3934–3937.
- Dolic, K., Siddiqui, A. H., Karmon, Y., Marr, K., & Zivadinov, R. (2013). The role of noninvasive and invasive diagnostic imaging techniques for detection of extra-cranial venous system anomalies and developmental variants. *BMC Medicine*, 11(1), 155.
- Sadad, T., Munir, A., Saba, T., & Hussain, A. (2018). Fuzzy C-means and region growing based classification of tumor from mammograms using hybrid texture feature. *Journal of Computational Science*, 29, 34–45.
- Fahad, H. M., Ghani Khan, M. U., Saba, T., Rehman, A., & Iqbal, S. (2018). Microscopic abnormality classification of cardiac murmurs using ANFIS and HMM. *Microscopy Research and Technique*, 81(5), 449–457. <https://doi.org/10.1002/jemt.22998>
- Fodor, I. K. (2002). A survey of dimension reduction techniques. In *Center for Applied Scientific Computing* (Vol. 9, pp. 1–18). Livermore, CA: Lawrence Livermore National Laboratory. <https://e-reports.ext.llnl.gov/pdf/240921.pdf>



- Haralick, R. M., Shanmugam, K., & Dinstein, I. (1973). Textural features for image classification. *IEEE Transactions on Systems, Man, and Cybernetics*, 3(6), 610–621.
- Houshmand, S., Werner, T., & Alavi, A. (2016). Molecular imaging of brain tumor: A review of available PET and MRI biomarkers. *Journal of Nuclear Medicine*, 57(Suppl. 2), 1235–1235.
- Hussein, Z. R., Rahmat, R. W., Nuriyana, L., Saripan, M. I., & Dimon, M. Z. (2009). Pre-processing importance for extracting contours from noisy echocardiographic images. *International Journal of Computer Science and Network Security (IJCSNS)*, 9(3), 134–137.
- Husham, A., Alkawaz, M. H., Saba, T., Rehman, A., & Alghamdi, J. S. (2016). Automated nuclei segmentation of malignant using level sets. *Microscopy Research and Technique*, Vol., 79(10), 993–997. <https://doi.org/10.1002/jemt.22733>
- Iqbal, S., Ghani, M. U., Saba, T., & Rehman, A. (2018). Brain tumor segmentation in multi-spectral MRI using convolutional neural networks (CNN). *Microscopy Research and Technique*, 81(4), 419–427. <https://doi.org/10.1002/jemt.22994>
- Iqbal, S., Khan, M. U. G., Saba, T., & Rehman, A. (2017). Computer assisted brain tumor type discrimination using magnetic resonance imaging features. *Biomedical Engineering Letters*, Vol., 8(1), 5–28. <https://doi.org/10.1007/s13534-017-0050-3>
- Jamal, A., Hazim Alkawaz, M., Rehman, A., & Saba, T. (2017). Retinal imaging analysis based on vessel detection. *Microscopy Research and Technique*, 80(17), 799–811. <https://doi.org/10.1002/jemt>
- Jain, R. K., & Schunck, B. G. R. (1995). *Machine vision* (Vol. 5). McGraw Hill.
- Jansen, M. (2012). *Noise reduction by wavelet thresholding* (Vol. 161). Berlin, Germany: Springer Science & Business Media.
- Kearns, M. (1997). A bound on the error of cross validation using the approximation and estimation rates, with consequences for the training-test split. *Neural Computation*, 9(5), 1143–1161.
- Kociotek, M., Materka, A., Strzelecki, M., & Szczypiński, P. (2001). *Discrete wavelet transform-derived features for digital image texture analysis*. Paper presented at the International Conference on Signals and Electronic Systems. pp. 99–104.
- Kumar, R. S., & Karnan, M. (2014). Review of MRI image classification techniques. *International Journal of Research Studies in Computer Science and Engineering*, 1(1), 21–28.
- Li, Q. Li, T. Zhu, S., & Kambhamettu, C. (2002). *Improving medical/biological data classification performance by wavelet preprocessing*. IEEE International Conference on Data Mining, 2003. pp. 657–660.
- Lone, T. A., & Malik, S. H. (2015). A comparative study of image Denoising techniques with special emphasis on medical images. *International Journal of Advance Foundation and Research in Science and Engineering*, 1(9), 10–18.
- Louis, D. N., Perry, A., Burger, P., Ellison, D. W., Reifengerger, G., von Deimling, A., ... Wesseling, P. (2014). International Society of Neuropathology-Haarlem Consensus Guidelines for Nervous System Tumor Classification and Grading. *Brain pathology*, 24(5), 429–435.
- Menze, Bjoern H., et al. (2015). The multimodal brain tumor image segmentation benchmark (BRATS). *IEEE Transactions on Medical Imaging*, 34(10), 1993–2024.
- Mittal, U., & Anand, S. (2013). Effect of morphological filters on medical image segmentation using improved watershed segmentation. *International Journal of Computer Science & Engineering Technology*, 1(4), 631–638.
- Mughal, B., Muhammad, N., Sharif, M., Saba, T., & Rehman, A. (2017). Extraction of breast border and removal of pectoral muscle in wavelet domain. *Biomedical Research*, 28(11), 5041–5043.
- Mughal, B., Sharif, M., Muhammad, N., & Saba, T. (2017). A novel classification scheme to decline the mortality rate among women due to breast tumor. *Microscopy Research and Technique*, 81, 171–180. <https://doi.org/10.1002/jemt.22961>
- Mughal, B., Muhammad, N., Sharif, M., Rehman, A., & Saba, T. (2018). Removal of pectoral muscle based on topographic map and shape-shifting silhouette. *BMC Cancer*, 18, 778. <https://doi.org/10.1186/s12885-018-4638-5>
- Nezamoddini-Kachouie, N., & Fieguth, P. (2005) *A Gabor based technique for image denoising*. Paper presented at the IEEE Canadian Conference on Electrical and Computer Engineering, 2005, pp. 980–983.
- Otsu, N. (1975). A threshold selection method from gray-level histograms. *Automatica*, 11(285–296), 23–27.
- Patil, S., & Udipi, V. R. (2012). Preprocessing to be considered for MR and CT images containing tumors. *IOSR Journal of Electrical and Electronics Engineering*, 1(4), 54–57.
- Paulinas, M., & Ušinskas, A. *A survey of genetic algorithms applications for image enhancement and segmentation*. Paper presented at the Information Technology and control 36.3 (2015).
- Perona, P., & Malik, J. (1990). Scale-space and edge detection using anisotropic diffusion. *IEEE Transactions on Pattern Analysis and Machine Intelligence*, 12(7), 629–639.
- Polesel, A., Ramponi, G., & Mathews, V. J. (2000). Image enhancement via adaptive unsharp masking. *IEEE Transactions on Image Processing*, 9(3), 505–510.
- Ramani, R., Vanitha, S. N., & Valarmathy, S. (2013). The pre-processing techniques for breast cancer detection in mammography images. *International Journal of Image, Graphics and Signal Processing*, 5.5, 47.
- Rehman, A., Abbas, N., Saba, T., Ijaz ur Rahman, S., Mehmood, Z., & Kolivand, K. (2018). Classification of acute lymphoblastic leukemia using deep learning. *Microscopy Research & Technique*, 81, 1310–1317. <https://doi.org/10.1002/jemt.23139>
- Rehman, A., Abbas, N., Saba, T., Mehmood, Z., Mahmood, T., & Ahmed, K. T. (2018). Microscopic malaria parasitemia diagnosis and grading on benchmark datasets. *Microscopic Research and Technique*. <https://doi.org/10.1002/jemt.23071>
- Rehman, A., Abbas, N., Saba, T., Mahmood, T., & Kolivand, H. (2018). Rouleaux red blood cells splitting in microscopic thin blood smear images via local maxima, circles drawing, and mapping with original RBCs. *Microscopic Research and Technique*, 81(7), 737–744. <https://doi.org/10.1002/jemt.23030>
- Saba, T., Rehman, A., Mehmood, Z., Kolivand, H., & Sharif, M. (2018). Image enhancement and segmentation techniques for detection of knee joint diseases: A survey. *Current Medical Imaging Reviews*, 14(5), 704–715. <https://doi.org/10.2174/1573405613666170912164546>
- Saba, T., Bokhari, S. T. F., Sharif, M., Yasmin, M., & Raza, M. (2018). Fundus image classification methods for the detection of glaucoma: A review. *Microscopy Research and Technique*, 81, 1105–1121. <https://doi.org/10.1002/jemt.23094>
- Simonetti, A. W., Melssen, W. J., van der Graaf, M., Postma, G. J., Heerschap, A., & Buydens, L. M. (2003). A chemometric approach for brain tumor classification using magnetic resonance imaging and spectroscopy. *Analytical Chemistry*, 75(20), 5352–5361.
- Travis, W. D. (2015). The 2015 World Health Organization classification of lung tumors: Impact of genetic, clinical and radiologic advances since the 2004 classification. *Journal of Thoracic Oncology* 10(9), 1243–1260.
- Vidyarthi, A. Agarwal, P., & Mittal, N. (2014) *Machine learning based classification of high grade malignant brain tumors using diverse feature set*. Paper presented at the 2nd International Conference on Advances in Computing and Information Technology (ICACIT), 2014.
- Vijaya, G., & Suhasini, A. (2014). An adaptive preprocessing of lung CT images with various filters for better enhancement. *Academic Journal of Cancer Research*, 7(3), 179–184.
- Wever, W. D., Coolen, J., & Verschakelen, J. A. (2011). Imaging techniques in lung cancer. *Breathe*, 7(4), 338–346.
- Yang, R., Sarkar, S., Korchinski, D. J., Wu, Y., Yong, V. W., & Dunn, J. F. (2016). MRI monitoring of monocytes to detect immune stimulating treatment response in brain tumor. *Neuro-oncology*, 19(3), 364–371.
- Yoon, H., Han, Y., & Hahn, H. (2009). Image contrast enhancement based sub-histogram equalization technique without over-equalization noise. *World Academy of Science, Engineering and Technology*, 50, 2009.
- Zhang, Y. J. (1996). A survey on evaluation methods for image segmentation. *Pattern Recognition*, 29(8), 1335–1346.
- Zuiderveld, K. (1994). *Contrast limited adaptive histogram equalization* (pp. 474–485). Graphics gems, San Diego, CA, USA.

**How to cite this article:** Tahir B, Iqbal S, Usman Ghani Khan M, et al. Feature enhancement framework for brain tumor segmentation and classification. *Microsc Res Tech*. 2019; 82:803–811. <https://doi.org/10.1002/jemt.23224>